Published in final edited form as:
J Mol Cell Cardiol. 2009 May ; 46(5): 695–703. doi:10.1016/j.yjmcc.2009.01.014.

Accelerated Inactivation of the L-type Calcium Current Due to a Mutation in CACNB2b Underlies Brugada Syndrome

Jonathan M Cordeiro, PhD[1], **Mark Marieb, MD**[2], **Ryan Pfeiffer, BSc**[1], **Kirstine Calloe, PhD**[3], **Elena Burashnikov, MSc**[1], and **Charles Antzelevitch, PhD**[1]

1 *Department of Experimental Cardiology, Masonic Medical Research Laboratory, Utica, NY, USA*

2 *Arrhythmia Center of Connecticut, New Haven, CT, USA*

3 *Danish Arrhythmia Research Center, University of Copenhagen, Copenhagen, Denmark*

Abstract

Background—Recent studies have demonstrated an association between mutations in *CACNA1c* or *CACNB2b* and Brugada syndrome (BrS). Previously described mutations all caused a loss of function secondary to a reduction of peak calcium current (I_{Ca}). We describe a novel *CACNB2b* mutation associated with BrS in which loss of function is caused by accelerated inactivation of I_{Ca}.

Methods and Results—The proband, a 32 yo male, displayed a Type I ST segment elevation in two right precordial ECG leads following a procainamide challenge. EP study was positive with induction of polymorphic VT/VF. Interrogation of implanted ICD revealed brief episodes of very rapid ventricular tachycardia. He was also diagnosed with vasovagal syncope. Genomic DNA was isolated from lymphocytes. All exons and intron borders of 15 ion channel genes were amplified and sequenced. The only mutation uncovered was a missense mutation (T11I) in *CACNB2b*. We expressed WT or T11I *CACNB2b* in TSA201 cells co-transfected with WT *CACNA1c* and *CACNA2d*. Patch clamp analysis showed no significant difference between WT and T11I in peak I_{Ca} density, steady-state inactivation or recovery from inactivation. However, both fast and slow decay of I_{Ca} were significantly faster in mutant channels between 0 and +20 mV. Action potential voltage clamp experiments showed that total charge was reduced by almost half compared to WT.

Conclusions—We report the first BrS mutation in *CaCNB2b* resulting in accelerated inactivation of L-type calcium channel current. Our results suggest that the faster current decay results in a loss-of-function responsible for the Brugada phenotype.

Keywords

genetics; ion channels; arrhythmia; calcium

Address for correspondence: Jonathan M Cordeiro, Ph.D., Masonic Medical Research Laboratory. 2150 Bleecker Street, Utica, NY 13501, Phone: (315) 735-2217 x132, Fax: (315) 735-5648, E-mail: jcordeiro@mmrl.edu, or Charles Antzelevitch, PhD, FAHA, Masonic Medical Research Laboratory, 2150 Bleecker Street, Utica, NY 13501, Tel. 315-797-6976 ext 117, Fax 315-735-5648, E-mail: ca@mmrl.edu.

Conflicts of Interest: None

INTRODUCTION

Brugada Syndrome (BrS) is characterized by an ST-segment elevation in the right precordial leads unrelated to ischemic or structural heart disease [1]. It is well established that mutations in *SCN5A*, the a-subunit of the cardiac Na^+ channel, reduce the magnitude of the cardiac Na^+ current by a variety of mechanisms [2] and are linked to the development BrS [3]. A second chromosome has been linked to the BrS in a large family in which the syndrome was also associated with progressive conduction disease, and a relatively good prognosis[4]. The gene was recently identified as the glycerol-3-phosphate dehydrogenase 1-like gene (*GPD1L*). The mutation in *GPD1L* has been shown to result in a reduction of I_{Na} [4,5]. Mutations in *SCN1B* ($Na_v\beta_1$)[6] have also recently been associated with BrS and shown to cause a loss of function of I_{Na}.

A recent study reported a mutation in ancillary subunit *KCNE3* in patients diagnosed with BrS [7]. Co-transfection of the *KCNE3* mutation with *KCND3* (Kv4.3, the pore forming a-subunit) resulted in a significant increase in the magnitude of the Ca^{2+}-independent transient outward current (I_{to}) compared to WT *KCNE3+KCND3*. Results of this study demonstrated a functional role of *KCNE3* (MiRP2) in the modulation of I_{to} in the human heart and suggested that mutations in *KCNE3* can underlie the development of BrS.

Blockade of the L-type Ca^{2+} channel (I_{Ca}) has been shown to lead to a BrS phenotype in isolated canine right ventricular wedge preparations [8]. Consistent with these findings, we identified a new clinical entity exhibiting ECG and arrhythmic manifestations of both BrS and short QT syndrome (SQTS) associated with loss of function mutations in the α1 (*CACNA1C*) and β (*CACNB2b*) subunits of the L-type cardiac calcium channel [9].

The balance of inward (typically I_{Na} and I_{Ca}) and outward (principally I_{to}) currents active during the early phase of the epicardial AP determine the magnitude of the AP notch and an outward shift in the balance of current can amplify the AP notch and predispose to loss of the AP dome, leading to the electrocardiographic and arrhythmic manifestations of BrS (for review see [10]). The outward shift can occur as a result of a reduction in the density or total charge of I_{Na} and I_{Ca} secondary to an accelerated inactivation of these currents. One of the first loss of function mutations in SCN5A associated with BrS was found to be due to an accelerated inactivation of the sodium channel [11]. A loss of function mutation associated with BrS due to accelerated inactivation of the L-type Ca^{2+} channel has as yet not been uncovered.

The cardiac L-type Ca^{2+} channel is believed to be comprised of a pore forming α_{1C}-subunit as well as ancillary α_2 and subunits [12]. The $_2$ subunit has been shown to enhance trafficking of the pore forming α_{1C}-subunit to the sarcolemmal membrane and to alter the biophysical properties of the channel [12,13]. Here we report the first Brugada syndrome mutation in the $_{2b}$ subunit of the L-type calcium channel (*CaCNB2b)* resulting in accelerated inactivation of I_{Ca} but not affecting trafficking. Our results suggest that the faster current decay results in a reduced total charge carried by I_{Ca} during the plateau of the action potential, thus predisposing to the BrS phenotype. Preliminary results have been presented as an abstract [14].

METHODS

ECG Measurement

The ECG was digitally scanned, magnified 4 to 8 times, and measured with digital calipers. The end of the T wave was defined as the intersection of a tangent, drawn to the descending portion of the T wave, with the isoelectric line.

Mutation Analysis

Genomic DNA was prepared from peripheral blood lymphocytes of patient (MMRL284) and available family members. All known exons of the principal BrS and candidate genes were amplified with intronic primers and sequenced in both directions to probe for mutations. The following genes were screened: *SCN5A, SCN1B, SCN3B, KCNH2, KCNQ1, KCNJ2, KCNE1, KCNE2, KCNE3, KCND3 (Kv4.3), KCNIP2 (KCHiP2), KCNJ11, CACNA1C, CACNB2b,* and *CACNA2D1*. No mutations were detected except in *CACNB2b.* All individuals studied in the control groups for the mutation, matched by race and ethnic background, were healthy and had no family history of cardiac arrhythmias based on written clinical history.

Cell Transfection/Mutagenesis

Site-directed mutagenesis was performed using QuikChange (Stratagene, LaJolla, CA) on full-length human wild type (WT) *CACNA1C* containing Exon 8A cDNA (accession number AJ224873) cloned in pcDNA3 [15,16]. *CACNA1C, CACNA2D1* and *CACNB2b* cloned in pcDNA3 were kind gifts from Dr. Nikolai Soldatov and Dr. Igor Splawski. TSA201 cells were grown in DMEM with Glutamax supplemented with 10% FBS in 35mm culture dishes and placed in a 5% CO_2 incubator at 37°C. To assess how T11I mutant channels altered the biophysical characteristics of I_{Ca}, TSA201 cells were co-transfected with a combination of mutant or WT *CACNB2b*. The cells were co-transfected using FuGene6 (Roche Diagnostics, Indianapolis, Ind) with a 1:1:1 molar ratio of WT human *CACNA1C*, WT or T11I mutant *CACNB2b*, and WT *CACNA2D1*. In addition, 0.40 μg of enhanced green fluorescent protein cDNA was added to the transfection mixture. Cells displaying fluorescence 48–72 h after transfection were used for electrophysiological study.

Measurement of Action Potentials

Single left ventricular myocytes were isolated from canine hearts using techniques previously described [17,18]. Action potentials of single cells were recorded using whole cell patch pipettes coupled to a MultiClamp 700A amplifier. The ventricular cells were superfused with a HEPES buffer of the following composition (mM): NaCl 126, KCl 4.0, $MgCl_2$ 1.0, $CaCl_2$ 2.0, HEPES 10, and glucose 11. pH adjusted to 7.4 with NaOH. The patch pipette solution had the following composition (mM): K-aspartate 90, KCl 30, glucose 5.5, $MgCl_2$ 1.0, EGTA 5, MgATP 5, HEPES 5, NaCl 10. pH = 7.2 with KOH. The resistance of the electrodes was 2–4 MΩ when filled with the pipette solution (described above). Action potentials were elicited using a 3 ms-current pulse at 120% threshold amplitude. Both Epi and Endo cells were paced at a cycle length of 0.5 Hz. The pre-recorded action potentials served as the waveforms for the AP clamp experiments. All myocyte recordings were made at 36±1° C.

The investigation conforms to the Guide for the Care and Use of Laboratory Animals published by the US NIH.

Electrophysiology

Voltage clamp recordings of I_{Ca} from transfected TSA201 cells were performed as previously described [15,9]. Briefly, patch pipettes were fabricated from borosilicate glass capillaries (1.5 mm O.D., Fisher Scientific, Pittsburgh, PA). The pipettes were pulled using a gravity puller (Narishige Corp., Tokyo, Japan) and filled with pipette solution of the following composition (mmol/L): 120 $CsCl_2$, 2.0 $MgCl_2$, 10 HEPES, 5 $CaCl_2$, 2 MgATP and 10 EGTA, pH 7.25 (CsOH). The pipette resistance ranged from 1–4 MΩ when filled with the internal solution. The perfusion solution contained (mmol/L): 130 NMDG, 5 KCl, 15 $CaCl_2$, 1 $MgCl_2$, 5 mM TEA-Cl, 10 HEPES, pH 7.35 with HCl. Current signals were recorded using a MultiClamp 700A amplifier (Axon Instruments Inc., Foster City, CA) and series resistance errors were

reduced by about 60–70% with electronic compensation. All recordings from TSA201 were made at room temperature.

Data Acquisition and Analysis

All signals were acquired at 20–50 kHz (Digidata 1322, Axon Instruments) with a microcomputer running Clampex 9 software (Axon Instruments, Foster City, CA). Voltage dependence of activation was measured from the current-voltage relation based on the equation: $I = G_{max} \cdot (V - V_{rev})/(1+\exp(-(V\ V_{1/2})/k)$, where I is the peak current amplitude, G_{max} the maximum conductance, V test potential, V_{rev} the reversal potential, $V_{1/2}$ the midpoint of activation, and k the slope factor. Steady-state was fitted to the Boltzmann equation, $I/I_{max} = 1/(1+\exp((V_m - V_{1/2})/k))$ to determine the membrane potential for half-maximal inactivation $V_{1/2}$ and the slope factor k. For all I_{Ca} recordings, the interpulse interval was 25 s to ensure full recovery and availability of channels. Membrane currents were analyzed with Clampfit 9 software (Axon Instruments, Foster City, CA). Results from pooled data are presented as Mean±SEM and n represents the number of cells in each experiment. Repeated measures ANOVA followed by Student-Newman-Keuls test or paired Student's t-test was used as appropriate for comparing paired data and a $p<0.05$ value was considered statistically significant.

RESULTS

The proband (MMRL284), a 34 year old male, experienced a syncopal attack and was seen in the ER but was discharged later that day. The following day, the patient still felt lethargic and again lost consciousness and was once again rushed to the ER. A preliminary ECG of patient showed ST segment elevation and negative T-wave in lead V1 (Figure 1A) and a QTc of 428 ms. Blood work revealed that CPK was elevated at 290 Units/liter. Upon procainamide infusion, the ECG of the patient became more consistent with a Brugada pattern with ST segment elevation in leads V1 and V2 (Figure 1B) and the QTc prolonged to 488 ms. After 1 gram of procainamide, patient had inducible VF and a shorter runs of polymorphic VT upon stimulation as well (Figure 1C). The father of the proband died at age 47 of an MI although the exact cause of death is questionable because he had substernal chest pain and felt poorly prior to collapsing and hitting his head and bleeding. Based on these findings and family history, he was implanted with an ICD. Subsequent follow-up interrogation of the ICD revealed 2 brief episodes of very rapid ventricular tachycardia (VT). Interestingly, the patient was also given the clinical diagnosis of vasovagal syncope.

Analysis of the patient's DNA showed a heterozygous C to T transition in exon 1 that predicted a substitution of threonine to isoleucine at position 11 (T11I) of *CACNB2b*, which was not present in 214 ethnically matched control alleles (Figure 2A). This mutation is located upstream of the -subunit interaction domain segment (Figure 2B), in variable domain 1 near the N-terminus [19].

To determine how the mutation in *CACNB2b* altered the biophysical properties of Ca^{2+} current and contributed to the clinical phenotype, we expressed calcium channels in TSA201 cells and performed patch clamp experiments. To compare the current-voltage (I–V) relationship between WT and the mutant channels, depolarizing pulses were applied to the cells in 10 mV increments from a holding potential of −90 mV. Both WT (Figure 3A) and T11I mutant channels (Figure 3B) showed substantial current under these recording conditions. Analysis of the current-voltage (I–V) relation of peak I_{Ca} showed that the current density was not significantly different between WT and T11I mutant channels (Figure 3C). The activation threshold and voltage eliciting peak current were similar for the WT and T11I channels, suggesting there were minimal differences in the activation or availability (Figure 3C). This was confirmed by analysis of steady-state activation, which showed mid-activation voltages

of +1.5±0.57 mV (n=12), and +3.5±0.49 mV, (n=13) for WT and T11I, respectively (p=NS, Figure 3D).

To probe for differences in steady state gating parameters between WT and T11I mutant channels, steady state inactivation of I_{Ca} was evaluated using a standard prepulse-test pulse voltage clamp protocol (Figure 4, top). The peak current following application of a 10 s pre-pulse to voltages between −100 and +20 mV was normalized to the maximum current and plotted as a function of the prepulse voltage to obtain the availability of the channels. Data were fitted to a Boltzman equation to determine the membrane potential for half-maximal inactivation $V_{1/2}$ and the slope factor k. Results showed a small but statistically significant shift in both steady-state inactivation and slope factor with mid-inactivation potentials of −24.8 ±0.46 mV, k=9.13±0.44 (n=13) for WT and −30.0±0.39 mV, k=6.25±0.31 (n=13) for T11I ($p<0.05$, Figure 4C). However, at normal cardiac membrane potentials both WT and mutant channels would exhibit full availability and it is unlikely that the difference in mid-inactivation would contribute to the clinical phenotype.

A double pulse protocol was used to examine recovery from inactivation (Figure 5). Representative traces of the frequency-dependent changes in I_{Ca} in WT and T11I channels are shown in Figure 5A and 5B. Recovery from inactivation of I_{Ca} at −90 mV was fit with a single exponential: τ = 101.4±3.7 ms for WT channels and τ =110.2±5.2 ms for T11I mutant channels (p=NS). The reactivation time course of I_{Ca} was similar for WT and mutant channels (Figure 5C).

Although peak I_{Ca} density was not significantly affected by the T11I mutation, the inactivation of the current appeared to be accelerated. WT channels exhibited a residual pedestal current as previously described [20] which appeared to be smaller or absent in the mutant. To confirm, we next analyzed the decay of the current by analyzing the inactivation kinetics of I_{Ca} current and produced by either WT- *CACNB2b* or T11I - *CACNB2b*. The decay of I_{Ca} (traces shown in Figure 3) elicited by pulses positive to −10 mV was fit with a bi-exponential function. Both the fast (Figure 6A) and slow (Figure 6B) time constants (τ) of decay were shorter for the mutated vs. WT channels at potentials between 0 and +20 mV ($p<0.05$). These results demonstrate that the T11I mutation in *CACNB2b* accelerates the inactivation kinetics of I_{Ca}.

To assess whether the accelerated inactivation of the mutated channels leads to a reduction in total charge during the action potential, we evaluated total charge carried by I_{Ca} by integrating the area under the current trace elicited by an action potential clamp using waveforms previously recorded from canine epicardial (Epi) or endocardial (Endo) cells (Figure 7). In response to the Endo AP waveform, WT currents (Figure 7A) and T11I (Figure 7B) displayed no significant differences in the magnitude or decay of I_{Ca}. We next integrated the current during the dome of the Epi AP waveform. The integrated current was evaluated from the lowest of the notch to the end of the action potential waveform. The amount of total charge during the plateau of the Epi action potential was 42±2.3% less in the T11I mutant compared to WT channels (n=5, $p<0.05$). The use of elevated Ca^{2+} improved signal-to-noise ratio in our current recordings but may have affected Ca^{2+}-dependent inactivation. Therefore, we performed the action potential clamp experiments under more physiological conditions (normal ionic concentrations at 36° C). The I_{Ca} recorded from WT channels following application of Epi and Endo waveforms (Figure 7D) closely resembled I_{Ca} recorded from myocytes under similar conditions [17,21]. At 36° C, WT and T11I currents displayed no significant differences in the magnitude or decay of I_{Ca} in response to the Endo AP waveform. However, the total charge during the plateau of the Epi action potential was 51±6.7% less in the T11I mutant compared to WT channels at 36° C (n=4, $p<0.05$). These observations confirm that the faster inactivation kinetics produced by T11I results in reduced depolarizing current contributing to the plateau of the epicardial action potential.

DISCUSSION

Mutations in *SCN5A* are known to reduce Na^+ current by a variety of mechanisms, leading to the development of BrS. One of the mechanisms includes accelerate inactivation of the cardiac Na^+ current [2,11]. In the present study, we have identified a case of BrS in which the disease phenotype was observed as a result of accelerated inactivation of the L-type Ca^{2+} current without significantly affecting peak current. The accelerated inactivation was due to a mutation in *CACNB2b*, which encodes the β subunit of the cardiac L-type Ca^{2+} current. The carrier of this mutation exhibited ST-segment elevation in only one precordial lead which converted to a more typical BrS phenotype with a procainamide challenge. VT/VF was inducible and subsequently detected upon interrogation of the implanted ICD, corroborating the diagnosis of a potentially life-threatening syndrome.

Alterations in L-type Ca^{2+} current have been implicated in the development of BrS both clinically [9] and experimentally [8]. However, in both studies the BrS phenotype was the result of a loss in peak I_{Ca}. In the present study, the BrS phenotype appears to be loss of function occurring as a result of accelerated inactivation of I_{Ca}, similar to the mechanism described for I_{Na} [11]. Moreover, results from the action potential clamp experiments suggest that cells with a prominent spike and dome morphology (i.e., epicardial and midmyocardial) would be affected to a greater degree compared to cells lacking a prominent phase 1 and having a consistently high plateau (i.e., endocardial cells or left ventricular cells). These cell type-specific differences are explained by the fact that inactivation of T11I channels was significantly faster at potentials negative to +20 mV (Figure 6). The presence of a spike and dome morphology therefore results in a greater degree of inactivation during the early phases of the action potential.

In the majority of cases involving loss of function of I_{Ca} previously reported, a new clinical phenotype was observed in which BrS characteristics were combined with a shorter than normal QT interval [9]. The proband in the present study presented with the ECG and arrhythmic manifestation of BrS, but with a normal QT interval (QTc=428 ms). This is likely due to the fact that cells in the left ventricle, which generally lack a prominent spike and dome morphology, are little affected by the accelerated inactivation of I_{Ca}.

Arrhythmogenesis in BrS is believed to be the result of amplification of heterogeneities in action potential characteristics among the different transmural cell types in the right ventricular myocardium [22,8]. A decrease in I_{Na} [23] or I_{Ca} [9] or augmentation of any one of a number of outward currents including I_{Kr} [24] or I_{to} [7] can cause preferential abbreviation of the right ventricular epicardial action potential, leading to the development of spatial dispersion of repolarization and thus the substrate and trigger for VT, which is usually polymorphic and less frequently monomorphic [25]. In the present study, we demonstrate that the T11I channels displays faster inactivation of I_{Ca} preferentially in the right ventricular epicardium resulting in reduced depolarizing current.

In a small minority of patients, BrS presents in conjunction with vasovagal syncope, as in the case of our proband. Whether this particular genotype contributes to this phenotypic expression is not known and could be the subject of future studies.

The functional role of Ca_v subunits is to promote trafficking of the subunit to the membrane [26], change the voltage dependence of channel activation and alter channel gating [13,27]. Evidence suggests that a 1:1 ratio of and subunits is necessary to form a functional L-type Ca^{2+} channel [28]. The importance of the N-terminal region of the $_2$ subunit to Ca^{2+} channel gating has been described previously. Biophysical analysis of 5 Ca^{2+} channel $_2$ splice variants that differed only in their amino terminal revealed dramatic differences in the rate of channel

inactivation. Consistent with that study, our mutation at position 11 of the $_2$ subunit resulted in accelerated inactivation of the Ca^{2+} current.

Recent PCR screening studies have uncovered a large diversity of Ca_v subunits in the human ventricle [29]. The $_{2b}$ isoform is thought to be the major isoform [26] with smaller amounts of other isoforms such as $_{1d}$ [30]. Immunocytochemical analysis of the localization and distribution of Ca_{v2} in ventricular myocytes showed a predominant T-tubular staining with some staining at the surface sarcolemma [29]. A similar staining pattern has been observed in ventricular myocytes for L-type Ca^{2+} channels [31] further demonstrating a functional interaction between and subunits. The importance of $_{2b}$ subunit in Ca^{2+} current inactivation was demonstrated by Gudzenko et al., who found that Ca^{2+}-induced inactivation was 83% complete in the presence of the $_{2b}$ subunit with a residual non-inactivating or pedestal current whereas in the absence of $_{2b}$, only 55% of the current inactivated [20]. WT current recorded in this study also exhibited a residual pedestal current which was absent in the T11I mutant. The absence of a pedestal current suggests less depolarizing current during the plateau of the action potential, an observation confirmed by AP clamp experiments (Figure 7).

Changes in action potential waveform and duration are known to affect excitation-contraction coupling [32,17,18]. In addition, it is well established that Ca^{2+} influx through L-type Ca^{2+} channels maintains the plateau of the action potential and initiates cardiac contractions [33]. However, the patients did not exhibit any impairment in cardiac output, presumably due to the fact that there was no reduction in QT interval or in peak I_{Ca}. In previous studies in which mutations in L-type Ca^{2+} channel were associated with a loss of current, no disruption in cardiac output was noted, suggesting compensatory mechanisms to preserve cardiac output [9]. For example, a greater proportion of the Ca^{2+} transient necessary for excitation-contraction coupling may be derived from the sarcoplasmic reticulum to compensate for reduced Ca^{2+} influx. Alternatively, there may be an upregulation of Ca^{2+} influx via other mechanisms, such as NCX [34,35].

Limitations of the Study

The results of our study show an acceleration of inactivation of L-type Ca^{2+} current. However, caution should be exercised when making the translation to the clinical setting. The TSA201 cells used in the present study expressed only the α, $_{2b}$, and $\alpha_2\delta$ subunits whereas cardiac myocytes likely have additional proteins which are not present in TSA201 cells. Some of these proteins include different β subunits as well as anchoring proteins, all of which combine to form the L-type Ca^{2+} channel [12]. It is likely that TSA201 cells are missing several key elements not present in the native myocytes. Although we clearly demonstrate that T11I produces accelerated inactivation of I_{Ca}, it is unclear to what extent the cardiac action potential duration would be affected due to the presence of other currents.

In summary, we have found a mutation in *CACNB2b*, the -subunit of the cardiac calcium channel in patient with BrS. Patch clamp analysis revealed that the mutation did not alter the magnitude of peak I_{Ca} but resulted in an acceleration of inactivation of L-type Ca^{2+} current. The accelerated inactivation of I_{Ca} translates into reduced depolarizing current preferentially in right ventricular Epi and M cells, which predisposes to the development of the Brugada phenotype. Thus, the results of the present study present a novel mechanism for the phenotypic expression of BrS.

Acknowledgements

We are grateful to Susan Bartkowiak for maintaining our Inherited Cardiac Arrhythmia Database and Judy Hefferon for assistance with the figures.

This study was supported by grants from the American Health Assistance Foundation (JMC), and US National Institutes of Health (NIH) grant HL47678 (CA).

Reference List

1. Brugada, Brugada. Right bundle branch block, persistent ST segment elevation and sudden cardiac death: a distinct clinical and electrocardiographic syndrome: a multicenter report. Journal of American College of Cardiology 1992;20:1391–6.
2. Chen, Kirsch, Zhang, Brugada, Brugada, Brugada, Potenza, Moya, Borggrefe, Breithardt, Ortiz-Lopez, Wang, Antzelevitch, O'Brien, Schultze-Bahr, Keating, Towbin, Wang. Genetic basis and molecular mechanisms for idiopathic ventricular fibrillation. Nature 3191998;392:293–6. [PubMed: 9521325]
3. Bezzina, Rook, Wilde. Cardiac sodium channel and inherited arrhythmia syndromes. Cardiovascular Research 212001;49:257–71. [PubMed: 11164836]
4. London, Michalec, Mehdi, Zhu, Kerchner, Sanyal, Viswanathan, Pfahnl, Shang, Madhusudanan, Baty, Lagana, Aleong, Gutmann, Ackerman, McNamara, Weiss, Dudley. Mutation in glycerol-3-phosphate dehydrogenase 1 like gene (GPD1-L) decreases cardiac Na^+ current and causes inherited arrhythmias. Circulation 11132007;116:2260–8. [PubMed: 17967977]
5. Van Norstrand, Valdivia, Tester, Ueda, London, Makielski, Ackerman. Molecular and functional characterization of novel glycerol-3-phosphate dehydrogenase 1 like gene (GPD1-L) mutations in sudden infant death syndrome. Circulation 11132007;116:2253–9. [PubMed: 17967976]
6. Watanabe, Koopmann, Le, Yang, Ingram, Schott, Demolombe, Probst, Anselme, Escande, Wiesfeld, Pfeufer, Kaab, Wichmann, Hasdemir, Aizawa, Wilde, Roden, Bezzina. Sodium channel β1 subunit mutations associated with Brugada syndrome and cardiac conduction disease in humans. J Clin Invest 2008;118:2260–8. [PubMed: 18464934]
7. Delpón, Cordeiro, Núñez, Thomsen, Guerchicoff, Pollevick, Wu, Kanters, Larsen, Burashnikov, Christiansen, Antzelevitch. Functional effects of *KCNE3* mutation and its role in the development of Brugada syndrome. Circ Arrhythm Electrophysiol 2008;1:209–18. [PubMed: 19122847]
8. Fish, Antzelevitch. Role of sodium and calcium channel block in unmasking the Brugada syndrome. Heart Rhythm 2004;1:210–7. [PubMed: 15851155]
9. Antzelevitch, Pollevick, Cordeiro, Casis, Sanguinetti, Aizawa, Guerchicoff, Pfeiffer, Oliva, Wollnik, Gelber, Bonaros, Burashnikov, Wu, Sargent, Schickel, Oberheiden, Bhatia, Hsu, Haissaguerre, Schimpf, Borggrefe, Wolpert. Loss-of-function mutations in the cardiac calcium channel underlie a new clinical entity characterized by ST-segment elevation, short QT intervals, and sudden cardiac death. Circulation 1152007;115:442–9. [PubMed: 17224476]
10. Antzelevitch. Brugada syndrome. Pacing and Clinical Electrophysiology 2006;29:1130–59. [PubMed: 17038146]
11. Dumaine, Towbin, Brugada, Vatta, Nesterenko, Nesterenko, Brugada, Brugada, Antzelevitch. Ionic mechanisms responsible for the electrocardiographic phenotype of the Brugada syndrome are temperature dependent. Circulation Research 10291999;85:803–9. [PubMed: 10532948]
12. Catterall, Perez-Reyes, Snutch, Striessnig. International Union of Pharmacology. XLVIII. Nomenclature and structure-function relationships of voltage-gated calcium channels. Pharmacological Reviews 2005;57:411–25. [PubMed: 16382099]
13. Morad, Soldatov. Calcium channel inactivation: possible role in signal transduction and Ca2+ signaling. Cell Calcium 2005;38:223–31. [PubMed: 16098584]
14. Cordeiro JM, Marieb M, Pfeiffer R, Calloe K, Burashnikov E, Antzelevitch C. Accelerated inactivation of the L-type calcium due to a mutation in CACNB2b underlies the development of a Brugada ECG phenotype. Circulation 10282008;118:S884–S885.Ref Type: Abstract
15. Splawski, Timothy, Sharpe, Decher, Kumar, Bloise, Napolitano, Schwartz, Joseph, Condouris, Tager-Flusberg, Priori, Sanguinetti, Keating. $Ca_V1.2$ calcium channel dysfunction causes a multisystem disorder including arrhythmia and autism. Cell 1012004;119:19–31. [PubMed: 15454078]
16. Splawski, Timothy, Decher, Kumar, Sachse, Beggs, Sanguinetti, Keating. Severe arrhythmia disorder caused by cardiac L-type calcium channel mutations. Proc Natl Acad Sci USA 672005;102:8089–96. [PubMed: 15863612]

17. Cordeiro, Greene, Heilmann, Antzelevitch, Antzelevitch. Transmural heterogeneity of calcium activity and mechanical function in the canine left ventricle. Am J Physiol Heart Circ Physiol 2004;286:H1471–H1479. [PubMed: 14670817]
18. Cordeiro, Malone, Di Diego, Scornik, Aistrup, Antzelevitch, Wasserstrom. Cellular and subcellular alternans in the canine left ventricle. Am J Physiol Heart Circ Physiol. 9282007
19. Van, Clark, Chatelain, Minor. Structure of a complex between a voltage-gated calcium channel beta-subunit and an alpha-subunit domain. Nature 6102004;429:671–5.
20. Gudzenko, Shiferaw, Savalli, Vyas, Weiss, Olcese. Influence of channel subunit composition on L-type Ca2+ current kinetics and cardiac wave stability. Am J Physiol Heart Circ Physiol 2007;293:H1805–H1815. [PubMed: 17545475]
21. Hund, Rudy. Rate dependence and regulation of action potential and calcium transient in a canine cardiac ventricular cell model. Circulation 11162004;110:3168–74. [PubMed: 15505083]
22. Yan, Antzelevitch. Cellular basis for the Brugada syndrome and other mechanisms of arrhythmogenesis associated with ST segment elevation. Circulation 10121999;100:1660–6. [PubMed: 10517739]
23. Vatta, Dumaine, Varghese, Richard, Shimizu, Aihara, Nademanee, Brugada, Brugada, Veerakul, Li, Bowles, Brugada, Antzelevitch, Towbin. Genetic and biophysical basis of sudden unexplained nocturnal death syndrome (SUNDS), a disease allelic to Brugada syndrome. Human Molecular Genetics 212002;11:337–45. [PubMed: 11823453]
24. Verkerk, Wilders, Schulze-Bahr, Beekman, Bhuiyan, Bertrand, Eckardt, Lin, Borggrefe, Breithardt, Mannens, Tan, Wilde, Bezzina. Role of sequence variations in the human *ether-a-go-go*-related gene (HERG, KCNH2) in the Brugada syndrome1. Cardiovascular Research 1212005;68:441–53. [PubMed: 16043162]
25. Antzelevitch, Brugada, Borggrefe, Brugada, Brugada, Corrado, Gussak, LeMarec, Nademanee, Perez Riera, Shimizu, Schulze-Bahr, Tan, Wilde. Brugada syndrome: report of the second consensus conference: endorsed by the Heart Rhythm Society and the European Heart Rhythm Association. Circulation 1172005;111:659–70. [PubMed: 15655131]
26. Colecraft, Alseikhan, Takahashi, Chaudhuri, Mittman, Yegnasubramanian, Alvania, Johns, Marban, Yue. Novel functional properties of Ca(2+) channel beta subunits revealed by their expression in adult rat heart cells. J Physiol 612002;541:435–52. [PubMed: 12042350]
27. Kobrinsky, Kepplinger, Yu, Harry, Kahr, Romanin, Abernethy, Soldatov. Voltage-gated rearrangements associated with differential β-subunit modulation of the L-type Ca^{2+} channel inactivation. Biophys J 2004;87:844–57. [PubMed: 15298893]
28. Dalton, Takahashi, Miriyala, Colecraft. A single CaVbeta can reconstitute both trafficking and macroscopic conductance of voltage-dependent calcium channels. J Physiol 9152005;567:757–69. [PubMed: 16020456]
29. Foell, Balijepalli, Delisle, Yunker, Robia, Walker, McEnery, January, Kamp. Molecular heterogeneity of calcium channel β-subunits in canine and human heart: evidence for differential subcellular localization. Physiol Genomics 4132004;17:183–200. [PubMed: 14762176]
30. Cohen, Foell, Balijepalli, Shah, Hell, Kamp. Unique modulation of L-type Ca2+ channels by short auxiliary beta1d subunit present in cardiac muscle. Am J Physiol Heart Circ Physiol 2005;288:H2363–H2374. [PubMed: 15615847]
31. Brette, Salle, Orchardm. Differential modulation of L-type Ca2+ current by SR Ca2+ release at the T-tubules and surface membrane of rat ventricular myocytes. Circulation Research 792004;95:e1–e7. [PubMed: 15192026]
32. Sah, Ramirez, Oudit, Gidrewicz, Trivieri, Zobel, Backx. Regulation of cardiac excitation-contraction coupling by action potential repolarization: role of the transient outward potassium current (I(to)). J Physiol 112003;546:5–18. [PubMed: 12509475]
33. Bers. Cardiac excitation-contraction coupling. Nature 1102002;415:198–205. [PubMed: 11805843]
34. Levi, Spitzer, Kohmoto, Bridge. Depolarization-induced Ca entry via Na-Ca exchange triggers SR release in guinea pig cardiac myocytes. Am J Physiol 1994;266:H1422–H1433. [PubMed: 8184920]
35. Litwin, Li, Bridge. Na-Ca exchange and the trigger for sarcoplasmic reticulum Ca release: studies in adult rabbit ventricular myocytes. Biophys J 1998;75:359–71. [PubMed: 9649393]

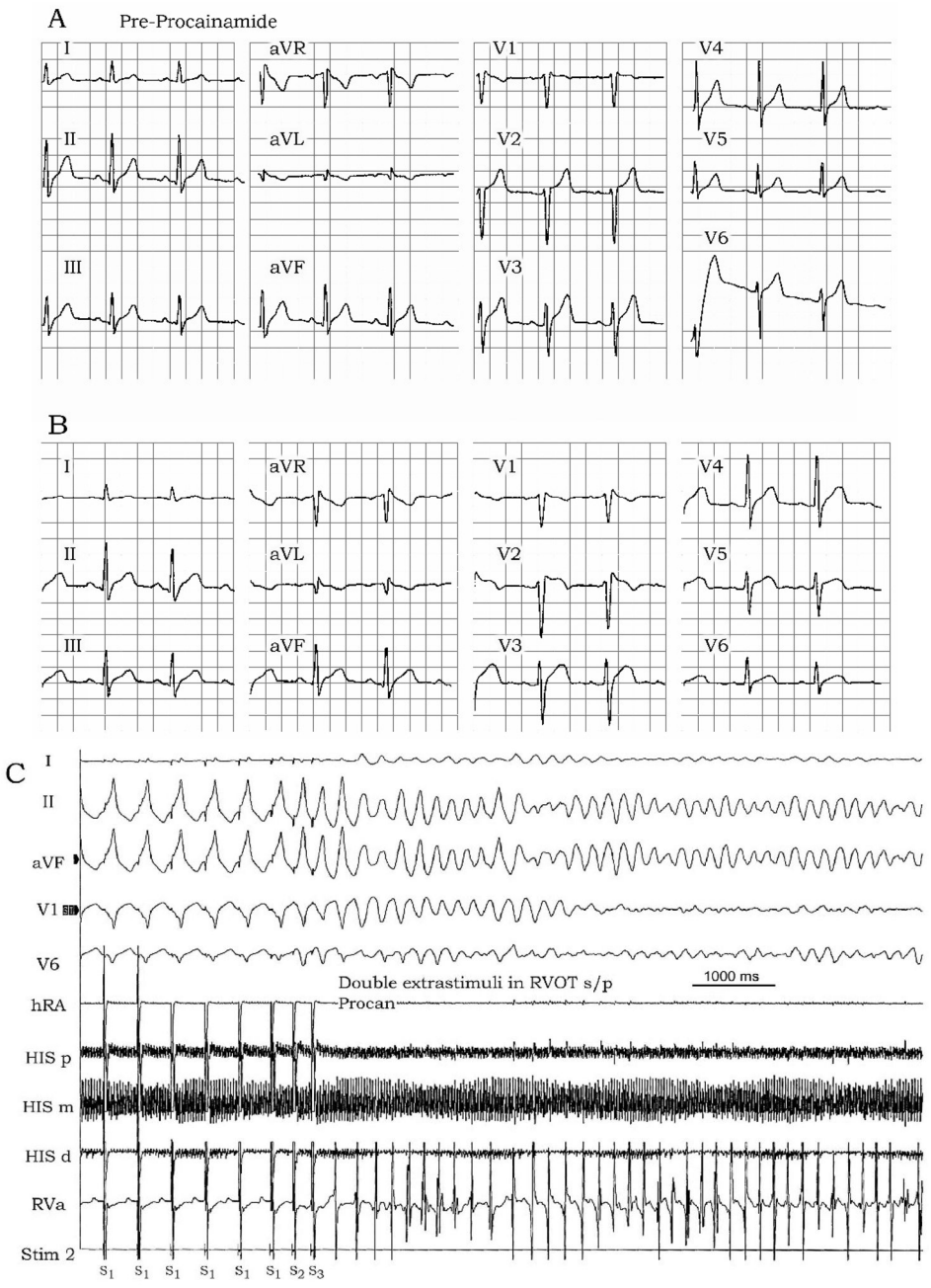

Figure 1.

Electrocardiograms of the patient. (**A**) Twelve-lead ECG of the patient at rest. ST-segment elevation and negative T-wave are present in one right precordial lead (V1). (**B**) After infusion of procainamide, a type ST segment elevation was apparent in V2 as well.. (**C**) Development of polymorphic ventricular tachycardia following programmed electrical stimulation (double extrastimuli).

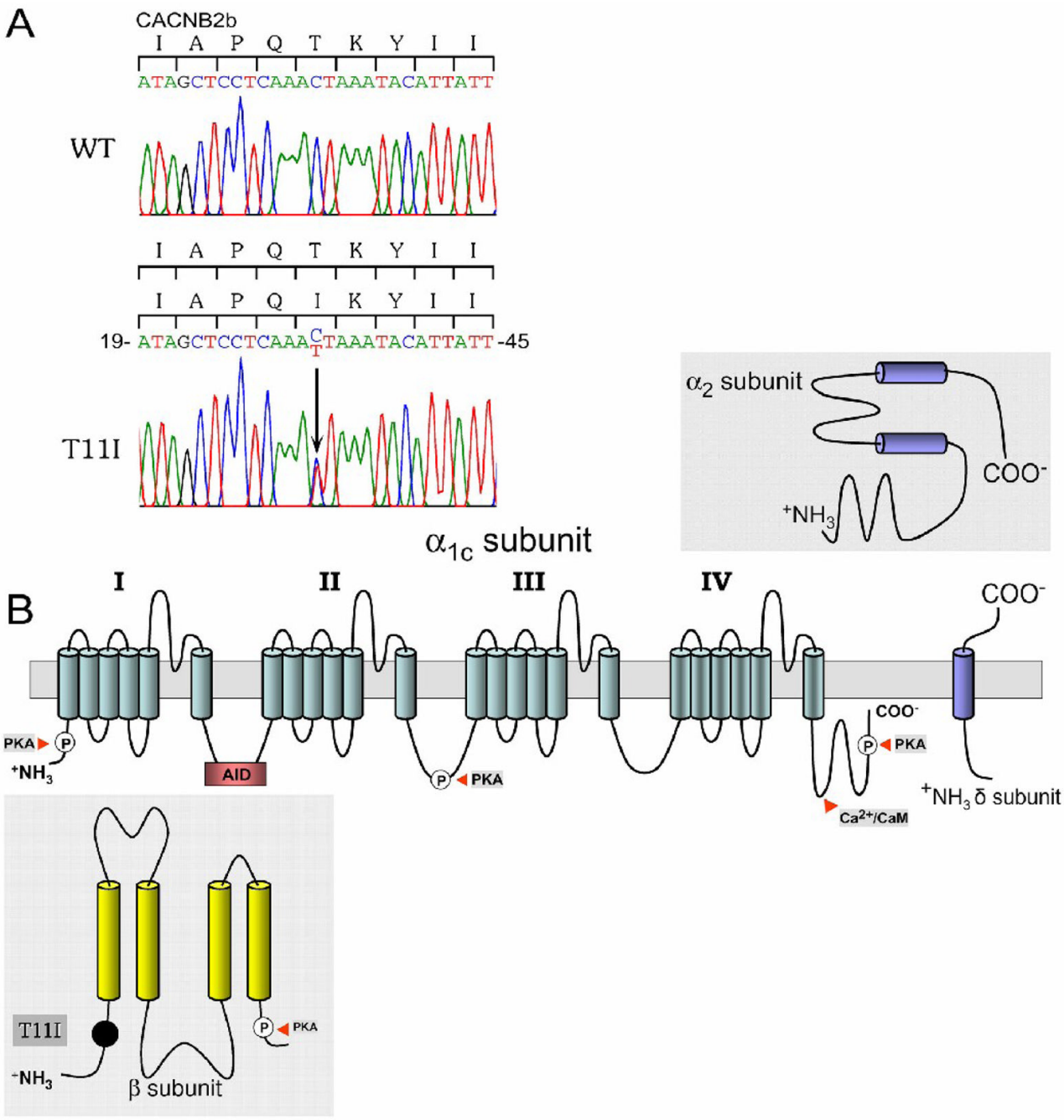

Figure 2.

A: DNA sequencing analysis. C to T substitution in exon 1 of *CACNB2b* predicts an amino acid substitution of threonine for lysine at codon 11 (T11I). **B:** Location of the T11I in the $-subunit of Ca_v 1.2. The cardiac Ca^{2+} channel α-subunit consists of four domains each containing six transmembrane-spanning segments.

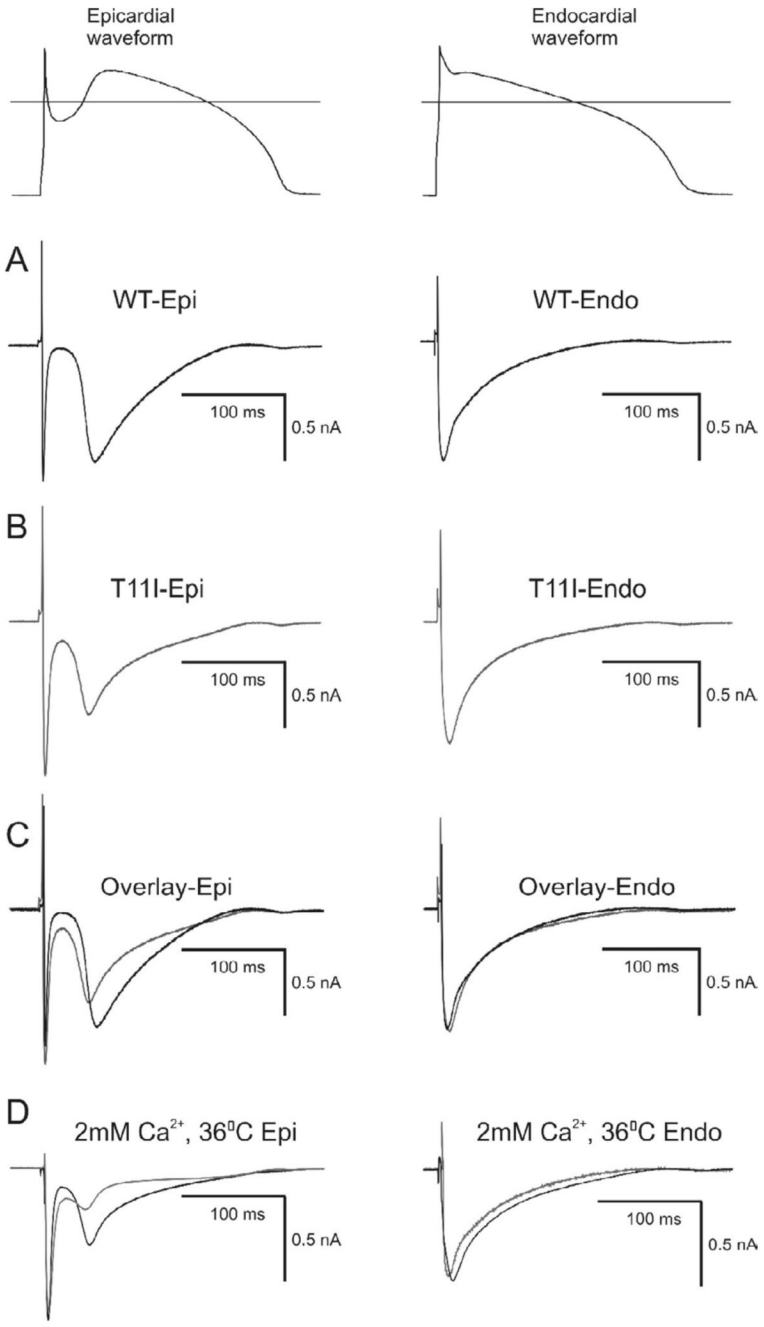

Figure 3.

Representative whole cell current recordings from a WT (**A**) and T11I mutant (**B**) expressed in TSA201 cells. Current recordings were obtained at test potentials between −50 and +60 mV in 10 mV increments from a holding potential of −90 mV. **C:** I–V relation for WT (n=12) and T11I (n=13) cells showing no statistically significant differences in peak calcium channel current density. **D:** Steady state-activation relation for WT and T11I. Chord conductance was determined using the ratio of current to the electromotive potential for the cells shown in Panel C. Data were normalized and plotted against their test potential.

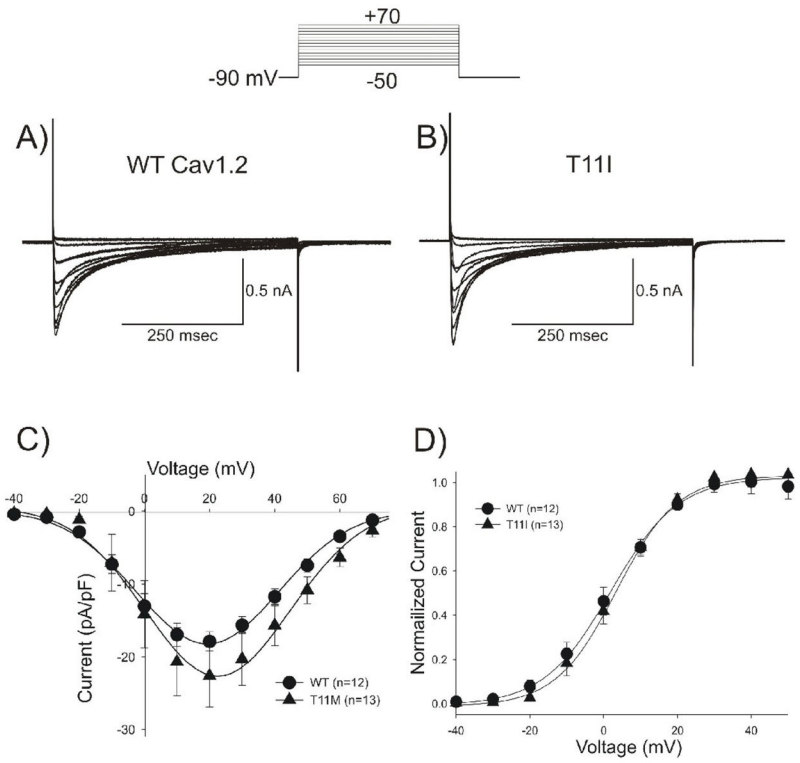

Figure 4.

Representative steady-state inactivation recordings for WT (**A**) and T11I (**B**) observed in response to the voltage clamp protocol shown at the top of the figure. **C:** Steady state-inactivation relation. Peak currents were normalized to their respective maximum values and plotted against the conditioning potential. T11I channels showed a mid-inactivation potential that was slightly but significantly hyperpolarized compared to WT channels.

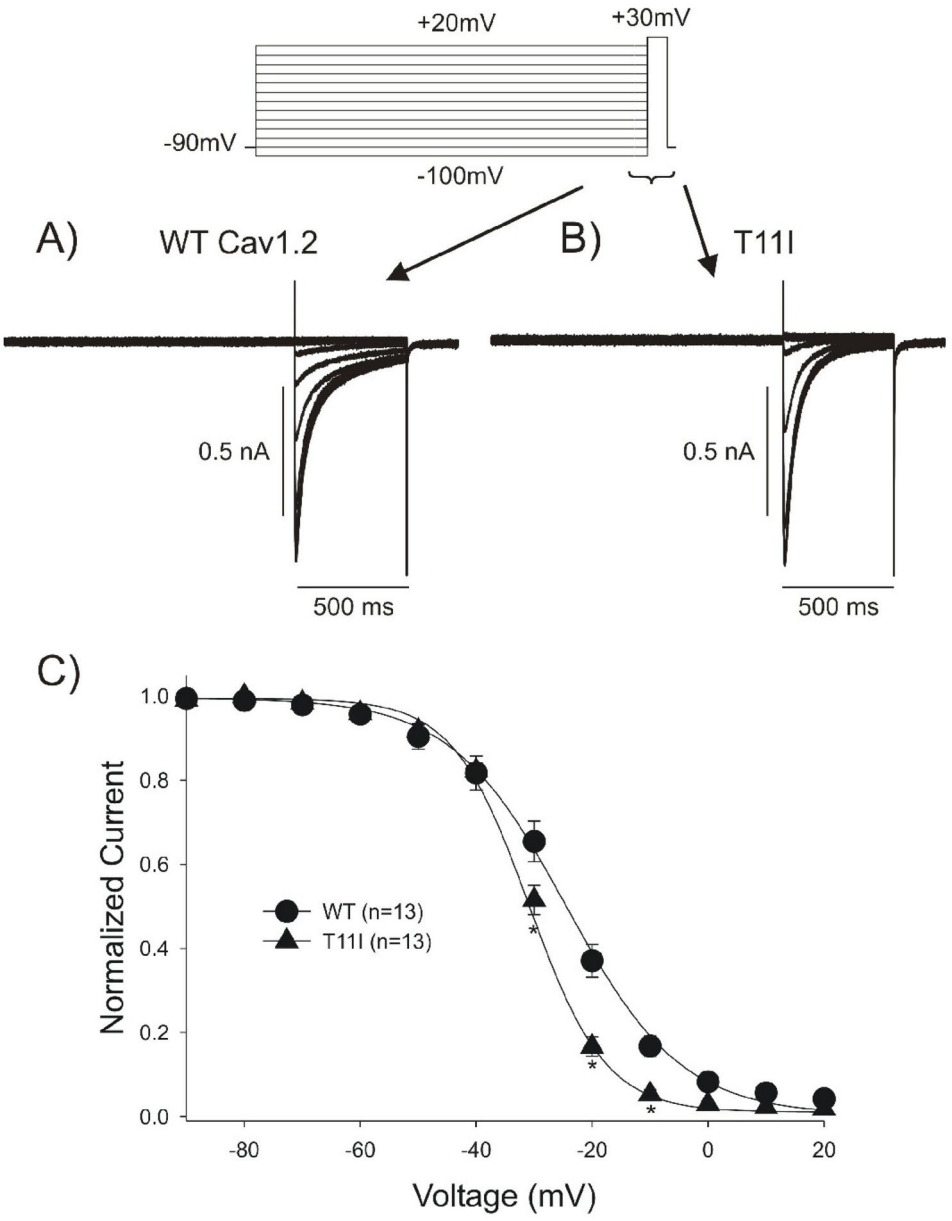

Figure 5.

Representative traces recorded from a WT (**A**) and T11I mutant (**B**) showing recovery of I_{Ca}. Recovery was measured using two identical voltage clamp steps to +20 mV from a holding potential of −90 mV separated by selected time intervals. Recovery time-course fit to a single exponential showed no difference in recovery rate between WT and T11I channels (**C**).

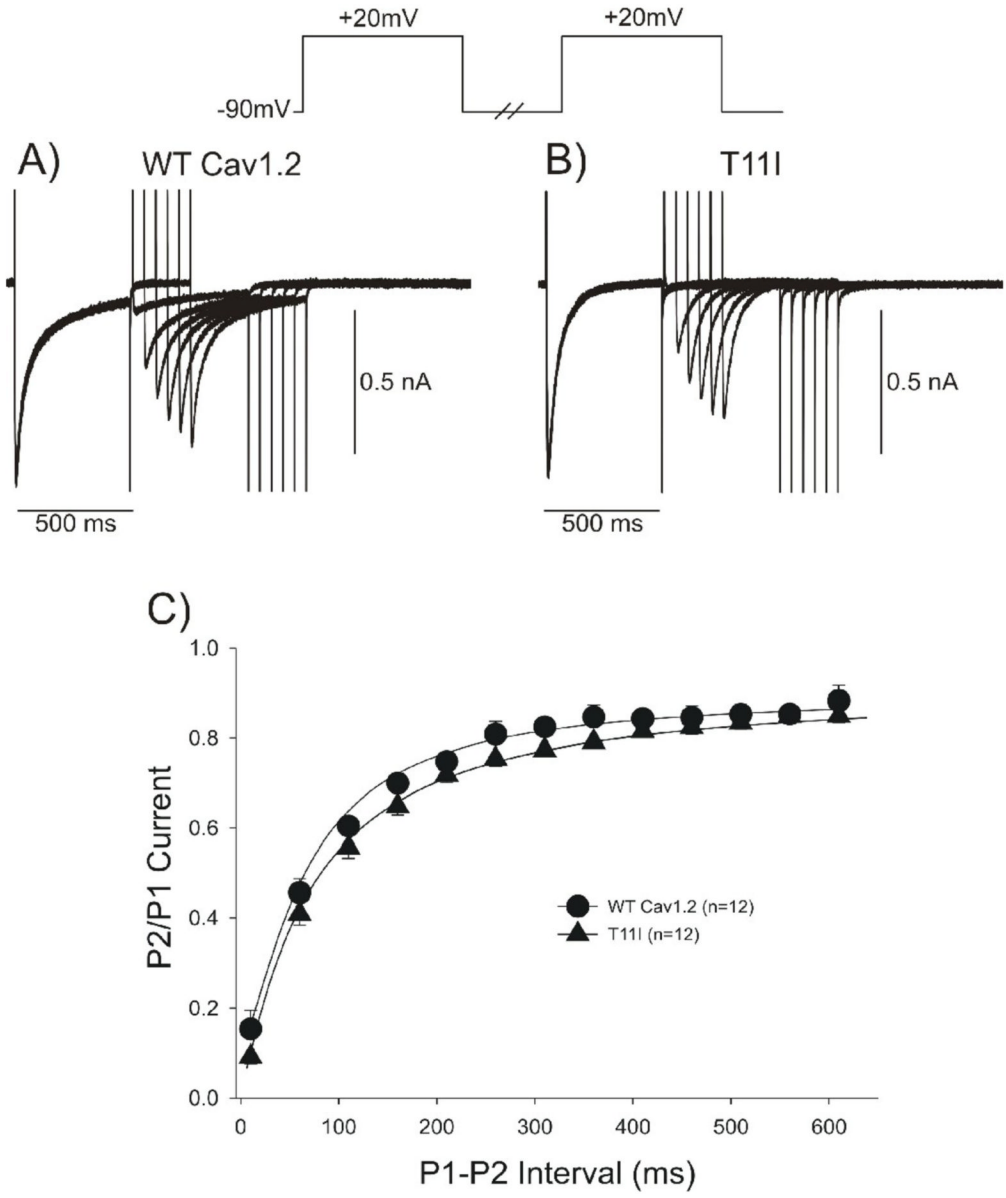

Figure 6.

A. Inactivation time constants (τ) for the fast phase of I_{Ca} decay as a function of voltage. Inactivation time constants (τ) values were measured by fitting a biexponential function to the current decay. *p<0.05 vs WT. **B:** Inactivation time constants (τ) for the slow phase of I_{Ca} decay as a function of voltage. *p<0.05 vs WT.

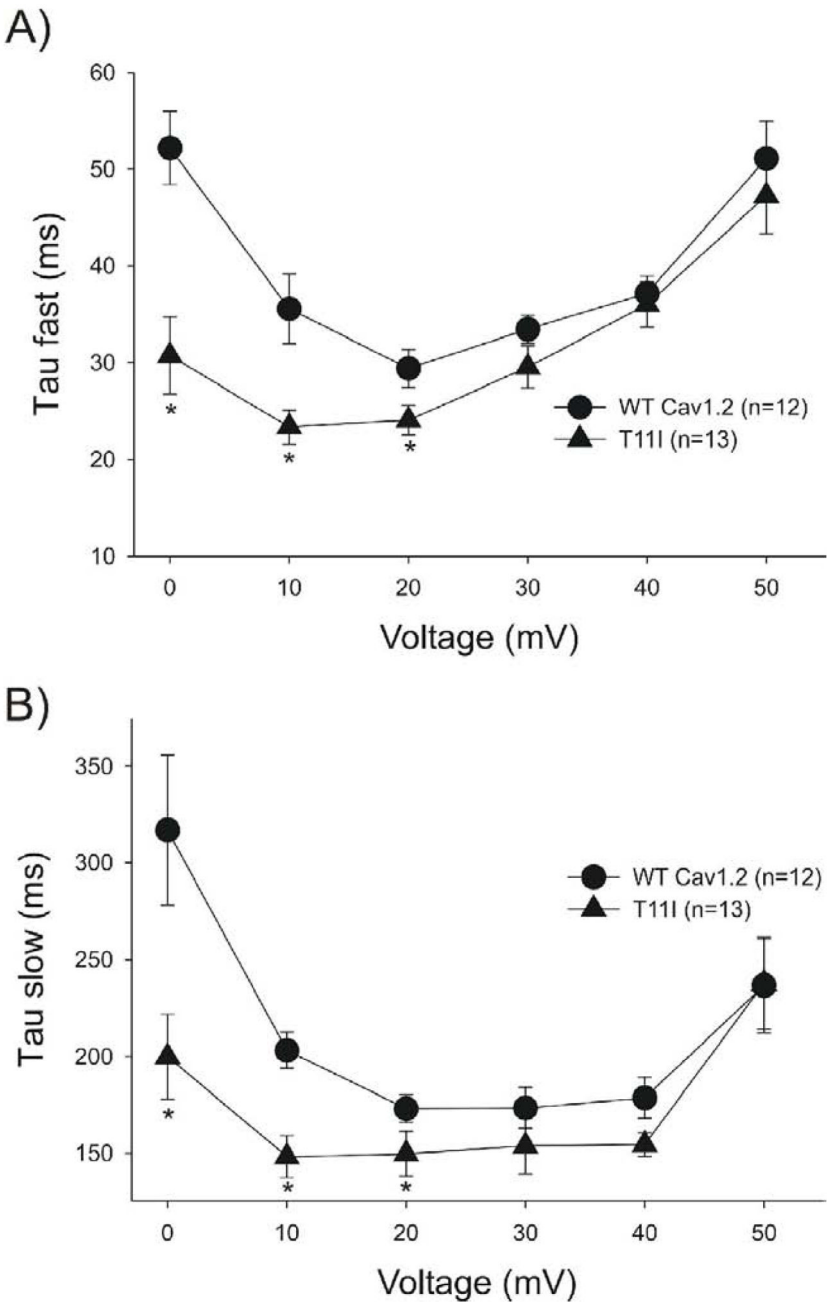

Figure 7.

Representative I_{Ca} currents elicited during action potential clamp experiments in TSA201 cells co-transfected with either WT or T11I *CACNB2b*. The action potentials were recorded from canine epicardial and endocardial cells which then served as the action potential clamp waveform (shown at top of figure). Horizontal line represents 0 mV. **A:** WT current traces following application of an epicardial and endocardial waveform. **B:** T11I currents following application of an epicardial and endocardial waveform. **C:** Superimposed current traces recorded from WT and T11I channels. Total charge during the plateau of the action potential was reduced by 42±2% (n=5) in T11I channels compared to WT when the epicardial waveform was applied. **D:** Superimposed current traces recorded from WT and T11I channels in 2 mM

Ca^{2+} external and 36° C. Total charge during the plateau of the action potential was reduced by 51±6.7% (n=4, $p<0.05$) in T11I channels compared to WT when the epicardial waveform was applied.